IJCSE International Journal of Computer Sciences and Engineering Open Access
Research Paper Vol.-7, Issue-10, Oct 2019 E-ISSN: 2347-2693

An Edge Based Technique for Spatially Varying Defocus Blur Estimation of Image using Gradient Magnitudes - Simulation & Result

Syed Faraz Ahmed Naqvi[1*], Kamal Niwaria[2], Bharti Chourasia[3]

[1,2,3]Dept. of Electronics & Communication Engineering, SRK University, Bhopal (MP) India

[*]*Corresponding Author: faraz_46200@yahoo.com, Tel.: 9755597335*

DOI: https://doi.org/10.26438/ijcse/v7i10.8189 | Available online at: www.ijcseonline.org

Accepted: 10/Oct/2019, Published: 31/Oct/2019

Abstract: The article presents a new edge based technique for spatially varying defocus blur estimation using a single image based on reblurred gradient magnitudes. Objects that do not lie at the focal distance of a digital camera generate defocused regions in the captured image. Also inherent dynamic characteristic of the nature gives rise to blur in captured image. Whenever there is relative motion between the object to be captured and the imaging system, the image captured at that instant is also suffered by blur. A locally adaptive scheme for obtaining the reblur scales, a connected edge filter for regularizing sparse map, and use of a fast guided filter for blur map propagation is suggested and simulated on Matlab. Results are compared and find to be performing bette in comparison with the older adopted technique.

Keywords*: Edge based technique, Blur estimation, Image processing, Gradient magnitude*

I. INTRODUCTION

Digital image are playing very vital role in soft application for industrial and corporate application such as bank, ERP, Automation and Security. Captured digital images inherit certain vulnerabilities & degradations [1]. The degradations may have many causes, but two types of degradations are often dominant: blurring and noise. Blurring is a form of bandwidth reduction of the image due to the imperfect image formation process. Image quality can refer to the level of accuracy in which different imaging systems capture, process, store, and compress, transmit and display the signals that form an image. Another definition refers to image quality as "the weighted combination of all of the visually significant attributes of an image". The difference between the two definitions is that one focus on the characteristics of signal processing in different imaging systems and the latter on the perceptual assessments that make an image pleasant for human viewers.

It can be caused by relative motion between the camera and the original scene, or by an optical system which is out of focus. When aerial photographs are produced for remote sensing purposes, blurs are introduced by atmospheric turbulence, aberrations in the optical system, and relative motion between the camera and the ground. Figure 1 shows a classical example of Blurred Image [2], [3].

Figure-1. Classical Example of Blurred Image

Blurring can be caused by relative motion between the camera and the original scene, or by an optical system which is out of focus [4]. When aerial photographs are produced for remote sensing purposes, blurs are introduced by atmospheric turbulence, aberrations in the optical system, and relative motion between the camera and the ground. Such blurring is not confined to optical images, for example, electron micrograph are corrupted by spherical aberrations of the electron lenses and Computed Tomographys scans suffer from X-ray scatter.

This is very clear that such a digital image cannot be used for image processing application, otherwise will not result in correct information.

II. IMAGE DEGRADATION

The term deblurring is commonly used to refer to restoration of images degraded by blur. Although the degradation

process is in general nonlinear and space varying, a large number of problems could be addressed with a Linear Shift Invariants (LSIs) model [4]. Because the output of an LSI system is the convolution of the true image with the impulse response of the system, the point spread function (PSF), image restoration in Linear Shift Invariant LSI systems is called image de-convolution. Typically, the phenomena of degradation is modeled as

$$g(x, y) = h(x, y) + \eta(x, y)$$

Where in the above expression following notations are used:
g(x;y) = Observed Degraded Image
f (x;y) = Original Image,
h(x;y) = Point spread function (PSF)
$\eta(x;y)$ = Noise present in the system
* = Convolution Operator used

Image Restoration is the operation of taking a corrupt or noisy image and estimating the clean, original image. The objective of image restoration techniques is to reduce noise and recover resolution loss. Image processing techniques are performed either in the image domain or the frequency domain [5]. The most straightforward and a conventional technique for image restoration is de-convolution, which is performed in the frequency domain and after computing the Fourier transform of both the image and the PSF and undo the resolution loss caused by the blurring factors. Also, conventionally the blurring process is assumed to be shift-invariant. Hence more sophisticated techniques, such as regularized deblurring, have been developed to offer robust recovery under different types of noises and blurring functions. This can be classified in three types: (1) Geometric Correction (2) Radiometric correction (3) Noise Removal.

Image restoration is widely used in almost all technical areas involving images; astronomy, remote sensing, microscopy, medical imaging, photography, surveillance, and High Definition Televisions systems [6]. The degraded images, generally, masks and blurs important but subtle features in the images. Other sources of blur degradation are geometric and motion un-sharpness. The geometric un-sharpness owes its origin from the lack of beam collimation, statistical fluctuation due to low intensities or high background. Similarly, motion un-sharpness is due to object motion during exposure, and limitations in acquisition or processing systems [7]. Hence, it becomes important to deblur the image which is subjected to aforementioned degradations.

To overcome these problems, image restoration is a solution to reduce the blurring effects on the image. It tries to perform an inverse transformation of the observed blurred image to estimate the original one. Modeling the degradation is an essential part in performing the inverse transformation.

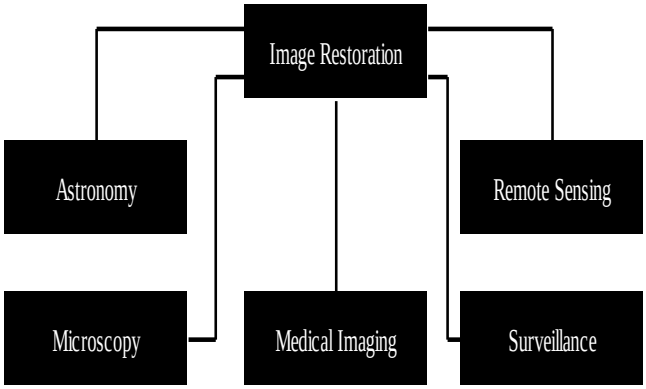

Figure-2. Applications of Image Restoration

III. DIGITAL IMAGE PROCESSING TECHNIQUES

Image quality attributes [8] are (1) **Sharpness**: determines the amount of detail an image can convey. System sharpness is affected by the lens design and manufacturing quality, focal length, aperture, and distance from the image center and sensor pixel count and anti-aliasing filter. (2) **Noise**: is a random variation of image density, visible as grain in film and pixel level variations in digital images. It arises from the effects of basic physics the photon nature of light and the thermal energy of heat inside image sensors. (3) **Color accuracy** is an important but ambiguous image quality factor (4) **Distortion** is an aberration that causes straight lines to curve (5) **Lens flare**, including "veiling glare" is stray light in lenses and optical systems caused by reflections between lens elements and the inside barrel of the lens.

A digital image can be considered as a matrix whose row and column indices represent point in the image and the corresponding matrix element known as picture element, pixels [9] value identifies the gray level at that point. The digital image processing takes as input an image always but the output can be an image or some relevant information retrieved after applying some function on the given input image. The improvement of pictorial information for human interpretation and processing of scene data for autonomous machine perception are the root application areas that had shown the interest in image processing field decades ago.

The various methods included as fundamental techniques of digital image processing are [10] **(1)** Image Representation **(2)** Modeling **(3)** Image Enhancement **(4)** Image Restoration **(5)** Image Analysis **(6)** Image Reconstruction **(7)** Image Data Compression.

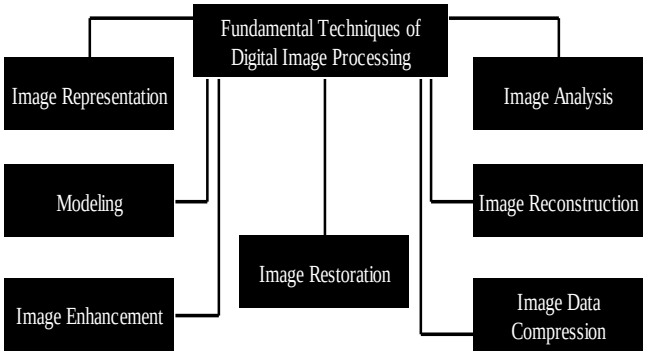

Figure-3. Fundamental Techniques of Digital Image Processing

IV. DEGRADED IMAGE RESTORATION PROCESS

The image processing technique dealt in this thesis is image restoration. Image restoration has been explored a lot till date but much has to be mined of still. From the wide broad spectrum of image restoration [11], only a part is worked out in this thesis, reconstruction of the true image and blurs parameter estimation. Figure 4 shows Image Degradation and Restoration Process applied in the commercial and industrial application.

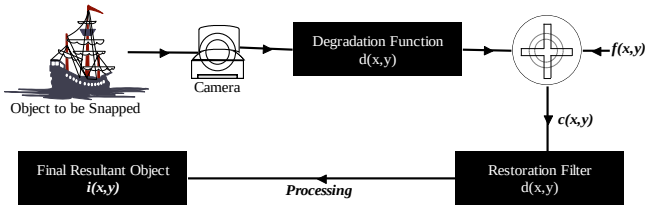

Figure-4. Image Restoration Process

Typically the research involved in the restoration of a degraded image can be classified as (1) non-blind and (2) blind methods. In the case of non-blind method, the PSF h(x;y) is assumed to be known and a sharp image can be induced from both the blurry image and the PSF [12].

Typical methods include the Richardson-Lucy method and Wiener filter. Ill-posedness is the most severe problem in image deblurring. In the case of non-blind deblurring, the observed blurred image g(x; y) does not uniquely determine the original image due to the ill-conditioned nature of the blur operator. This means that if there is a slight mismatch between the assumed PSF and the true PSF, or if the observed blurred image is corrupted by noise, the recovered image may be much worse than the underlying original image f (x; y). Driven by these problems and the fact that in most situations of practical interest the PSF, is not known with good accuracy, blind methods for restoring the degraded image are introduced in the literature. The task of simultaneously estimating the PSF and deblurring [13] an unknown image using partial or no information about the imaging system is known as blind image restoration. This problem is highly ill-posed since there are an infinite set of image-blur pairs that can synthesize the observed blurry image. In recent years, many novel approaches have been introduced to handle both the non-blind and blind deblurring problem, driven by a various motivations.

V. IMAGE RESTORATION PROBLEM FORMULATION

The image is characterized by two major components (1) Illumination (2) Reflectance Components [14]. But, practically apart from these two components, the image formation also depends on the characteristics of the object being captured, environmental conditions during capture, and the imaging system being used. These other components produce an ill-effect during image acquisition to produce a degraded image. The process of reconstructing the original scene from a degraded version is the goal of image restoration. The ill-effect causing functions, df is known as the blur. The additive noise effect is also considered as another cause of degradation [15]. Thus, the image degradation model is,

$$c = d_f i + \eta$$

Given c, some knowledge about the degradation function $\boldsymbol{d_f}$, and some knowledge about the additive noise term $\boldsymbol{\eta}$, the objective of restoration is to obtain an estimate $\boldsymbol{i'}$ of the original image. This estimate, $\boldsymbol{i'}$, should be as close as possible to the original input image. In general, the more knowledge we have about $\boldsymbol{d_f}$ and $\boldsymbol{\eta}$, the closer $\boldsymbol{i'}$ will be to $\boldsymbol{i}$. Figure below shows the image degradation and restoration process.

Image restoration refers to removal or minimization of known degradations in an image. The process includes de-blurring of images degraded by the limitations of a sensor or its environment, noise filtering, and correction of geometric distortion or non-linearity due to sensors. The image restoration had found its break through application in the engineering community in the area of astronomical imaging. Due to rapidly changing index of refraction of the atmosphere, ground-based imaging systems were subject to blurring. Extraterrestrial observations of the earth and the planets were degraded by motion blur as a result of slow camera shutter speeds relative to rapid space-craft motion. Till today, key focus area of image restoration is astronomical imaging. Another challenging area where image restoration plays a very important part is in the area of medical imaging. The use of digital techniques to restore aging and deteriorated films is also important and well-known application area of image restoration. Digital image restoration is being used in many other applications as well, say, for example, lastly but not the least, to improve federal aviation inspection procedures, restoration has been used to restore blurry X-ray images of air craft wings [16].

In blind image de-convolution, an observed image ***c(x; y)***, is assumed to be the two dimensional convolution of the true image ***i(x; y)*** with a linear-shift invariant blur , known as point spread function, PSF, ***d(x; y)*** and the additive noise is assumed zero.

$$c(x,y) = i(x,y) * d(x,y)$$

The problem of reconstructing the true image ***i(x; y)*** requires the de-convolution of the PSF, ***d(x; y)*** from the degraded image, ***i(x; y)***. A lot of research has been done exploring the various methods for image de-convolution as blind techniques. But still, is a critical and challenging problem for the researcher [17].

The convolved signals that is the true image and the ***psf*** are irreducible. This is the most important characteristic for the unambiguous de-convolution. The true image or ***psf*** should not be resultant of convolution of two or more other independent different component signal. Let us assume the following assumption true image that is ***i***, ***i(x; y) = i1(x; y)*** and $i_2(x; y)$ and ***psf, d(x; y) = d1(x; y) * d2(x; y),*** then the image model can be re-written as below:

$$c(x,y) = i_1(x,y) * i_2(x,y) * d_1(x,y) * d_1(x,y)$$

Hence, the deconvolution would be ambiguous as its quite difficult to clearly classify the true image component and the ***psf*** component.
The blind image de-convolution produces the scaled, shifted version of the true image [18]. So,

$$i' = Ai(x - b_1, y - b_2)$$

Where:
A, b_1, b_2 are arbitrary real constants and i' is the estimation of original image. This shifted and scaled version is again treated using some other information as support constraint to further improve the result. But the blind de-convolution cannot find A, b_1, b_2.

The main objectives of presented article are **(1)** To develop an algorithm in moment domain for restoring the blurred images using Minimization techniques **(2)** Blurred image restoration by estimating the PSF parameters

Digital Image Blur can be explained as the phenomenon of fading of boundaries of image or sharp point defecation due to different technical or operational issues taken from digital camera.

Digital image blur can basically classified in two most basic categories (1) Motion Blur (2) Out of Focus Blur. These are tow most applied basic categories which are frequently used in different image processing application in industrial and commercial applications.

Motion blur is the apparent streaking of moving objects in a photograph or a sequence of frames, such as a film or animation. It results when the image being recorded changes during the recording of a single exposure, due to rapid movement or long exposure.

The out of focus blur is seen when a camera pictures an image and object which are out of focus will be seen as faded figure result in quality degradation of digital image.

Figure-5. Motion blurred regions (left) & out-of-focus blurred regions (right)

Point Spread Function PSF
The degradation producing ill-effect of blur is termed as the point spread function, psf. Any type of blur is characterized by the psf . The electromagnetic radiation or other imaging waves propogated from a point source or point object is known as the psf. The quality of any imaging system depends on the degree of spreading (blurring) of the point object. The psf defines the impulse response of a point source. This is shown in Figure 2.1. When an image is captured by any recording system, the intensity of a pixel of the recorded image is directly proportional to the intesity of the corresponding section of the sight be captured. But this is ideal situation. Practically, the recorded intensity either gets effect by the noise or blur.

The psf causing degradation of any image are often two types as (1) Spatial-variant blur (2) Spatial-invariant blur.
For example, if the scene contains two objects moving with different velocities to the recording system, then the ***psf*** is effectively different for each. Also in the case of original Hubble Space Telescope Wide-field or Planetary camera, due to errors in the shaping of the mirrors, the ***psf*** has a large amount of spatial variati [19]. The image restoration in space-invariant case is done by deconvolving the observed image with psf.

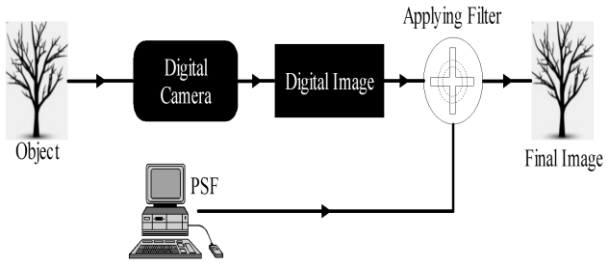

Figure-6. Image Enhancement Process

Motion Blur: The moving objects when captured by the camera or the stationary object captured by moving camera cause motion blur. Many types of blur has been framed out in the literature. This can be in the form of a translation, a rotation, a sudden change of scale or to some combination of these. But, here only the translation is considered. When the object is moving with a constant velocity V is being captured by the camera with an exposure time interval [0 T], the distortion is given by below equation:

$$d(x,y,s,t) = \begin{cases} \frac{1}{VT}\delta(y-t) & 0 \le (x-s) \le VT \\ 0 & otherwise \end{cases}$$

Out-of-focus Blur: When a sight is captured by the camera in a two-dimensional field, it may happen that some parts are in focus while other parts are not. The degree of defocus depends upon the effective lens diameter and the distance between the object and the camera. This leads to the point-spread function:

$$d(x,y) = \begin{cases} \frac{1}{\pi r^2} & if\ (x^2+y^2) \le r^2 \quad 7 \\ 0 & otherwise \end{cases}$$

In the equation 4.1, r is radius of circle of confusion.

Atmospheric Turbulence Blur: The blur occurred due to the long-exposure through the atmosphere in certain application is modelled as the ***gaussian psf***. The ***psf*** in this case is given as:

$$d(x,y) = Kexp\left(-\frac{x^2+y^2}{2\sigma^2}\right)$$

Gaussian Blur

The image degradation due to atmospheric condition is modelled by the gaussian effect. The gaussian blur is a type of image blurring filter that uses normal distribution for calculating the transformation to apply to each pixel in the image. The visual effect of this blurring is a smooth blur resembling that of viewing the image through the translucent screen. The apparent ”wobbling” distortion of scene when viewed through an open fire or across a hot road is well-known phenomenon. Similar effects are seen in the astronomical imaging also.

The visualization and characterization of the effect is of considerable interest to atmospheric scientists, earth-based astronomers and also for long-range surveillance. The deconvolution techniques are required for proper analysis in the scientific study.

VI. DIGITAL BLIND DEBLURRING

A digital blurred image or distorted image passes through different steps in order to enhance the quality of the image by deblurring the image using estimated PSF. In first step the image is captured using digital camera and stored in digital format in system [20]. The PSF which is needed to be used for the specific image first needed to be calculated by observation of the image status. Image estimation is done in objective to calculate PSF for specific image using selected algorithm. Then PSF is used to find deblurred image in blind condition. The flow chart is as shown in the figure below.

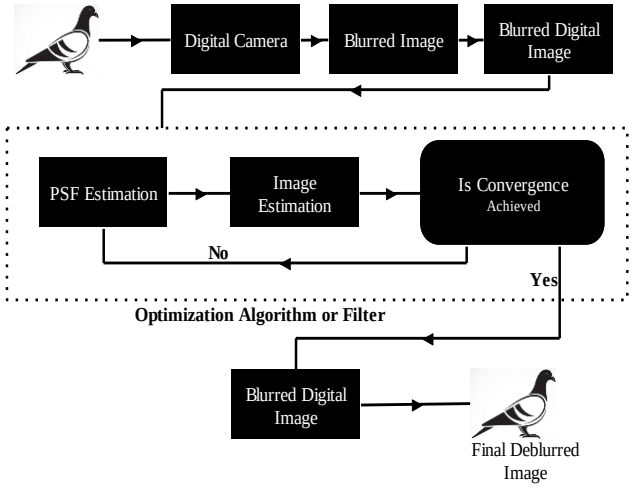

Figure-7. Digital Image Deblurring in Blind Deblurring Process.

VII. BLURRED IMAGE RESTORATION TECHNIQUE

In the article, the estimation of the Gaussian PSF is carried out using the Weighted Geometric moments that is WGM. Weighted Geometric moments works as an effective edge descriptor which together with extreme learning machine that is ELM is used for the estimation of PSF parameters. The estimation performance of the ELM using cross-database analysis performed on different standard databases. This is followed by restoration in moments domain and reconstructing the restored image using 2D cascaded digital filters operating as subtractors. To validate, the suggested technique, experimental work has been carried out on databases and results is compared with existing methods. The results obtained using the proposed method demonstrates effectiveness of method compared to existing methods.

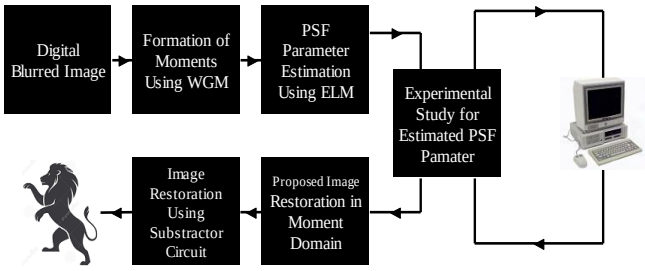

Figure-4.1. Blurred Image Restoration Technique Steps

We mainly focus on problem of image deblurring. Image deblurring is an inverse problem where the objective is to

recover a sharp image from its degraded version affected due to various distortions such as atmospheric turbulence, optical aberrations, sensor or motion blur.

Weighted Geometric Moments (WGM) based feature vectors formation

Tchebichef moments are well known edge descriptors of an image. Using the information geometric moments is expressed in terms of Tchebichef moments we can calculate the feature vectors image under consideration for restoration. Tchebichef moments can be used for edge detection.

Using the relationship between the Tchebichef moments and Geometric Moments, a set of weighted Geometric moments (WGM) can be derived and used for edge detection. The weighted Geometric moments (WGM) is defined as below:

$$WGM_{pq} = \sum_{k=0}^{p} \alpha(p, N{:}K) \sum_{i=0}^{q} \alpha_2(q, N{:}K) \sum_{i=0}^{k} \sum_{j=0}^{l} s_k^i \, s_l^i m_{ij}$$

The proposed weighted geometric moments (WGM) are defined as below:

$$WGM_{01} = Am_{00} + Bm_{01}$$
$$WGM_{10} = Am_{00} + Bm_{10}$$
$$WGM_{02} = Cm_{00} + Dm_{01} + Em_{02}$$
$$WGM_{10} = Cm_{00} + Dm_{10} + Em_{20}$$
$$WGM_{03} = Fm_{00} + Gm_{01} + Hm_{02} + Im_{03}$$
$$WGM_{30} = Fm_{00} + Gm_{10} + Hm_{20} + Im_{30}$$

Weighted Geometric Moments (WGM) as edge descriptors

By employing these WGM's for edge description, it will certainly encode the PSF information in a similar way as Tchebichef moment did. Now, the applicability of these WGM for the estimation of PSF parameters is elaborated.

Here, the characteristics of WGMs defined in equation 4.6 to - 4.10 for various types of edge contributions i.e. horizontal, vertical or diagonal present in an image is explored. This is done because edges provide vital information for humans to subjectively quantify the sharpness of the image. For this the proposed feature vector is as follows:

$$F = [\beta_1 \quad \beta_2 \quad \beta_3 \quad \beta_4]$$

Where in the above expression:

$$\beta_i = \sqrt{\mathrm{WGM}_{oi}^2 + \mathrm{WGM}_{io}^2} \text{ for } i = 1,2,3,4$$

The advantage of using the feature vector ***F*** is that it can characterize not only horizontal and vertical edges but also the diagonal edges as well. This is explained by studying the behavior of the feature vector F for varying degree of Gaussian ***PSF*** parameter s by selecting the random patches of size ***8X8*** from the Cameraman image.

One of the important characteristic in choosing the features for estimating the degree of blurriness in an image is that they should closely exhibit human visual system ***(HVS)*** perception of image blur distortion. It can be observed from Figure 4.5 that the components of the feature vector F decreases monotonically with the increase in ***PSF*** parameter ***s***. This is in accordance with the correlation between the human subjective score with the sigma s for the ***LIVE*** image database. The same holds true for most of the natural images present in other databases also.

To ensure the better generalization ability of the ELM network, the optimal selection of the hidden neurons, the corresponding input weights (W) and bias values (B) are required. Performance of the ELM depends on the proper selection of the hidden neurons, input weights and bias values. A selection of these parameters is crucial for proper generalization by ELM. In the proposed work, ELM network with 80 hidden neurons is considered. ELM algorithm is called 500 times for the same and cross database training/testing data and finds the mean and variance of the testing and training accuracies. Each time the ELM is called, the fixed parameters, namely weights (W) and bias (B) are initialized randomly from a uniform distribution. The input feature vectors are normalized between 0 to 1 and the weights (W) and bias (B) are initialized between 1. Here, the unipolar sigmoidal activation function for the hidden neurons is opted.

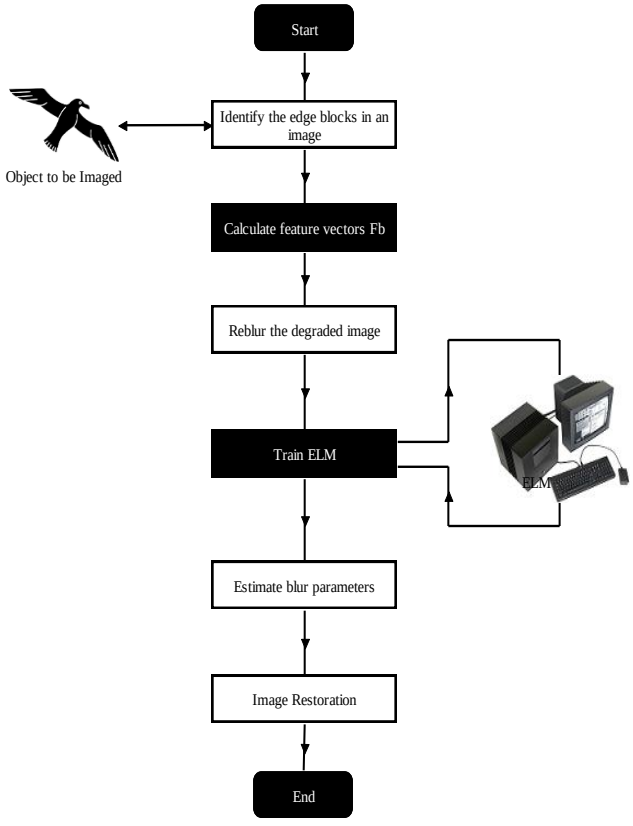

Figure 8. flowchart of proposed algorithm to estimate PSF parameters

Simulation is the imitation of the operation of a real-world process or system. The act of simulating something first

requires that a model be developed; this model represents the key characteristics, behaviors and functions of the selected physical or abstract system or process. The model represents the system itself, whereas the simulation represents the operation of the system over time.

MATLAB that is Matrix Laboratory is a multi-paradigm numerical computing environment. A proprietary programming language developed by Math Works, MATLAB allows matrix manipulations, plotting of functions and data, implementation of algorithms, creation of user interfaces, and interfacing with programs written in other languages, including C, C++, C#, Java, Fortran and Python. Although MATLAB is intended primarily for numerical computing, an optional toolbox uses the MuPAD symbolic engine, allowing access to symbolic computing abilities. An additional package, Simulink, adds graphical multi-domain simulation and model-based design for dynamic and embedded systems. As of 2017, MATLAB has roughly 1 million users across industry and academia. MATLAB users come from various backgrounds of engineering, science, and economics. MATLAB supports developing applications with graphical user interface that is GUI features. MATLAB includes GUIDE that is GUI development environment for graphically designing GUIs. It also has tightly integrated graph-plotting features. MATLAB can call functions and subroutines written in the programming languages C or FORTRAN.

VIII. SIMULATION SETUP AND RESULTS

In this study, images are taken from six publicly accessible databases for training and testing of the proposed algorithm in order to estimate the PSF parameters: LIVE, CSIQ, CIDIQ, TID2009, Caltechand Berkeley. Here, original images from all the databases are used. The images in all the databases vary in terms of its content and size. These images are successively degraded using PSF with varying sigma (s) and size (w) thus producing sample images to be used for training and testing of the proposed algorithm.

Range of Parameter in Experimental Test Setup is as specified below:

1. σ = sigma (s) = varies from 0.3 to 4 in steps of 0.1
2. ω = size (w) = Varies from 7x7 to 17x17 in steps of 2x2.

Table-1. Details of testing & training samples for various databases

Database	Original Image	Total Image	Training	Testing
LIVE	29	6612	4600	2012
CIDIQ	23	5244	3670	1574
CSIQ	30	6840	4788	2052
Berkeley	32	7296	5107	2189
TID2008	25	5700	3990	1719
Caltech	34	7752	5425	2327

The details of the original images present in all the databases along with the number of images used for training and testing are shown in Table-1. Table-2 shows the detail breakdown of the selected images into edge and plain blocks. Images are arranged in Table 5.2 with decreasing contribution of edges. This is done to observe the performance of the proposed algorithm on images with varying edge contribution.

Table-2: Classification of LIVE database images based on image content

Images	Plain	Edge
Building	3%	97%
Painted House	31%	69%
Light House	51%	49%
Parrots	85%	15%

Two experiments are conducted which are based on cross database of Berkeley dataset images are used for training the ELM while testing is performed using LIVE database images mentioned in Table 5.2. In the first experiment, only the edge blocks of the image are considered for training while in the second experiment, both the plain and edge blocks of the image are used for training the ELM. The estimation of the PSF parameters (σ and ω) obtained using ELM for both the experiments are shown in Tables 3 and 4. The estimation of σ for both the experiments along with their relative errors defined as $(x_0 - x)/x$ where x_0 is the measured and x is the true value is shown in Table 3 for different images.

Table-3. Edge block role in estimating PSF sigma for Images of Building, Light House & Painted House

Image	σ	Edge **Estimated σ**	Edge+ Plains **Estimated σ**
Building	0.5	0.51	1.51
	1.0	0.99	2.14
	3.5	3.51	2.84
Light House	0.5	0.52	1.24
	1.0	1.04	0.78
	3.5	3.65	4.12
Painted House	0.5	0.52	1.12
	1.0	1.05	2.54
	3.5	3.45	3.12

A similar experiment to estimate the PSF size (ω) is carried out and shown in Table 5.4. It can be observed that by considering the edge blocks of an image, the proposed algorithm closely estimates the PSF size. On the other hand the error increases in the estimation of PSF size (ω) if both the edge and plain blocks are considered.

Table-4. Edge block role in estimating PSF size (ϖ) for Images of Building, Light House & Painted House

Image	ϖ	Edge **Estimated ϖ**	Edge+ Plains **Estimated ϖ**
Building	5X5	7X7	11X11
	9X9	11X11	13X13
	17X17	17X17	11X11
Light House	5X5	5X5	13X13
	9X9	7X7	3X3
	17X17	17X17	7X7
Painted House	5X5	5X5	13X13
	9X9	11X11	3X3
	17X17	15X15	9X9

Estimating the PSF parameters is essential to obtain a good quality image, for which ELM is used. The evaluation is done using 10 runs. In this validation scheme, for each run, a random partition is done by selecting 70% of the data for testing while the remaining 30% as training. This is motivated by a similar method adopted in recent state of the art methods for cross validation analysis of estimated parameters. Once each run is done, the performance of the regression analysis is carried in terms of correlation coefficient (CC). Once the ELM is trained, the performance of the proposed method is evaluated from the same database. This can clearly be observed from above table that correlation coefficients values for all databases are in the range.

IX. SIMULATION RESULTS

Simulation in MATLAB is done using optimization technique to establish a relationship between actual σ and estimated σ. The Simulation graphs are as depicted below in the figures below:

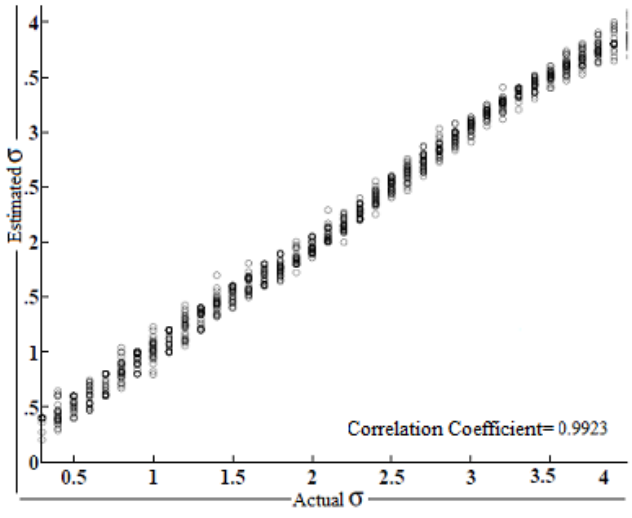

Figure-9. Correlation between actual σ and estimated σ for Dataset Image Building

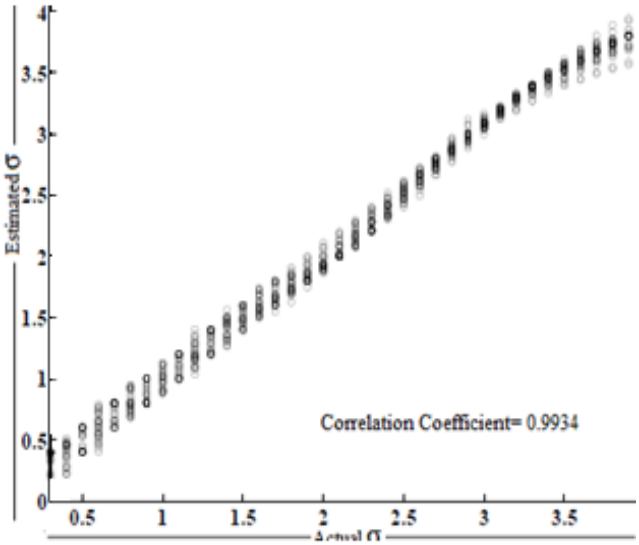

Figure-10. Correlation between actual σ and estimated σ for Dataset Image Light House

The test simulation is done in the Matlab-7.0 Software and had been done using Matlab code window. The test simulation cod is attached in the Appendix of the report. Simulation Tests are performed using the blurred images of the LIVE database to evaluate the performance of the proposed method with the three existing methods. In the first experiment four images from the LIVE database that vary in image content. Further, visual quality of the two images is shown to demonstrate the effectiveness of the proposed approach. In the second experiment, a comparative analysis of the 29 original images blurred with specific pairsis shown in terms of SSIM scores. Further, analysis of the proposed method with the images used in the existing methods is carried out to have a fair comparison in terms of SSIM scores.

In the test simulation we had conducted comparison on Light House Image with Kotera Restoration, Goldstein Restoration and G. Liu Restoration to the proposed technique with different PSM.

In order to measure the effectiveness of the proposed method with the existing ones, a fair comparison in terms of the restoration is performed using the images present in the existing methods. The restoration results obtained by proposed method are based on the training of ELM using Berkeley database and testing using the images taken from Kotera Technique & Goldstein Technique. Table 5.5 presents the comparative analysis of the restoration performed on the blurred images. It can be observed that the proposed method provides a satisfactory restoration results when compared to the other existing technique.

Table-5. Numerical Comparative Simulation Results

Image	Actual (σ, ω)	Estimated (σ, ω)	SSIM			
			Proposed Restoration	Kotera Restoration	Goldstein Restoration	G.Liu. Restoration
Parrots	(0.5,7)	(0.54, 7)	0.9692	0.9594	0.9487	0.9332
	(2.5,13)	(2.34, 13)	0.8732	0.9108	0.8486	0.8271
Building	(0.5,7)	(0.51, 5)	0.9742	0.9645	0.9567	0.9357
	(4.0,17)	(4.11,17)	0.8067	0.8145	0.7767	0.7512
Light House	(1.0,9)	(1.04,7)	0.9331	0.9236	0.9125	0.8926
	(4.0,17)	(4.16, 17)	0.7832	0.8178	0.7843	0.7721
Paint House	(1.0,9)	(1.05, 11)	0.9456	0.9303	0.9278	0.9272
	(1.5,11)	(1.48, 11)	0.9165	0.9015	0.8996	0.8732

Table-6. De-blurring in different images in percentage (%)

Image	Set Index (σ, ω)	De-blurring in %			
		Proposed Restoration	Kotera Restoration	Goldstein Restoration	G.Liu. Restoration
Parrots	Set_1	96%	95%	94%	93%
	Set_2	97%	91%	84%	82%
Building	Set_1	97%	96%	95%	93%
	Set_2	80%	81%	77%	75%
Light House	Set_1	93%	92%	91%	89%
	Set_2	78%	81%	78%	77%
Paint House	Set_1	94%	93%	92%	92%
	Set_2	91%	90%	89%	87%

X. CONCLUSION

Following important aspect can be concluded on the basis of the above result:

1. The proposed Technique is of significant importance as the percentage of deblurring is considerable improved.
2. The improvement in the deblurring percentage depends upon the quality of the image selected for assignment.
3. The improvement in the deblurring percentage depends upon the ω factors.
4. The performance of technique depends upon the Training of ELM and the database feeded to the same at the time of training.
5. PSF estimation plays an important role in the final result hence this is mandatory to uses advance technique for PSF estimation.

REFERENCES

[1] A M Deshpande, S Patnaik, "Single image motion deblurring: An accurate PSF estimation and ringing reduction[J]", Optik-International Journal for Light and Electron Optics, vol. 125, no. 14, pp. 3612-3618, 2014.

[2] N. Phansalkar, "Determination of linear motion point spread function using hough transform for image restoration," in Proc. 2010 IEEE Int. Conf. Computational Intelligence and Computing Research, Coimbatore, India, 2010, pp. 211-224.

[3] L. Yuan, J. Sun, L.Quan, and H. Y. Shum, "Image deblurring with blurred/noisy image pairs," ACM Trans. Graphics, vol. 26, article no. 1, 2007, pp:120-129.

[4] Q. Shan, J. Jia, A. Agarwal, "High-quality motion deblurring from a single image," ACM Trans. on Graphics, vol. 27, article no. 73, 2008, pp:1130-1145

[5] M. Cannon, "Blind deconvolution of spatially invariant image blurs with phase," IEEE Trans. Acoust. Speech Signal Process., vol. 24, pp. 56-63, 1976.

[6] M. M. Chang, A. M. Tekalp, and A. T. Erdem, "Blur identification using the bispectrum," IEEE Trans. Signal Process., vol. 39, pp. 2323-2325, 1991.

[7] J. Biemond, R. L. Lagendijk, and R. M. Mersereau, "Iterative methods for image deblurring," Proc. of the IEEE, vol. 78, pp. 856-883, 1990.

[8] C. Mayntz, T. Aach, and D. Kunz, "Blur identification using a spectral inertial tensor and spectral zeros," IEEE image Process., vol. 2, pp. 885-889, 1999.

[9] F. Krahmer, Y. Lin, B. Mcadoo, K. Ott, J. Wang, D. Widemann, and B. Wohlberg, "Blind image deconvolution: Motion blur estimation," IMA Preprints Series, 2006.

[10] N. Norouzi, and M. E. Moghaddam, "Motion blur identification using image derivative," in Proc. 2008 IEEE Int. Conf. Signal Processing and Information Technology, Sarajevo, Yugoslavia, 2008, pp. 380-384.

[11] M. E. Moghaddam, and M. Jamzad, "Motion blur identification in noisy images using mathematical models and statistical measures," Pattern Recognition, vol. 40, pp. 1946-1957, 2007. pp:1921-1934

[12] R. Dash, P. K. Sa, and B. Majhi, "RBFN based motion blur parameter estimation," in Proc. 2009 IEEE Int. Conf. Advanced Computer Control, Singapore, Singapore, 2009, pp. 327-331.

[13] C. C. Liebe, "Accuracy performance of star trackers-a tutorial", IEEE Trans. Aerosp. Electron. Syst., vol. 38, no. 2, pp. 587-599, 2002.

[14] T Sun, F Xing, Z You et al., "Smearing model and restoration of star image under conditions of variable angular velocity and long exposure time [J]", Optics express, vol. 22, no. 5, pp. 6009-6024, 2014

[15] T Sun, F Xing, Z You et al., "Motion-blurred star acquisition method of the star tracker under high dynamic conditions [J]", Optics express, vol. 21, no. 17, pp. 20096-20110, 2013.

[16] M Dobes, L Machala, T Fürst, "Blurred image restoration: A fast method of finding the motion length and angle[J]", Digital Signal Processing, vol. 20, no. 6, pp. 1677-1686, 2010.

[17] "Pattern analysis with two-dimensional spectral localization: Applications of two-dimensional S transforms" by L. Mansinha R. G. Stockwell , R. P. Lowe in Physica A vol. 239 pp. 286-295 IEEE-2017

[18] "Space-local spectral texture map based on MR images of MS patients" by H. Zhu, Mayer, Mansinha L. A, Law C. J. Archibald, Luanne J. R in Mitchell MS: Clin. Lab. Res. IEEE-2018

[19] W Hou, H Liu, Z Lei et al., "Smeared star spot location estimation using directional integral method [J]", Applied optics, vol. 53, no. 10, pp. 2073-2086, 2014.

[20] T Sun, F Xing, Z You et al., "Smearing model and restoration of star image under conditions of variable angular velocity and long exposure time [J]", Optics express, vol. 22, no. 5, pp. 6009-6024, 2014.

